

## CHAPTER II

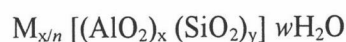
### THEORY

#### 2.1 Molecular Sieves for Use in Catalytic Reaction

In 1932, McBain proposed the term “molecular sieve” to describe the class of materials that exhibited selective adsorption properties. The molecular sieve must separate components of a mixture on the basis of shape and size differences. The class of molecular sieve now includes the silicates, the metasilicates, metalloaluminates, the  $\text{AlPO}_4$ 's, and silico- and metalloaluminophosphates. The different classes of molecular sieve materials are listed in Figure 2.1.

#### 2.2 Structure and Properties of Zeolites

Structurally, the zeolite is microporous molecular sieves that is a crystalline aluminosilicate with a framework based on an extensive three-dimension network of the oxygen ions. Located within the tetrahedral sites formed by the oxygen can be either a  $\text{Si}^{4+}$  or an  $\text{Al}^{3+}$  ion. The  $\text{AlO}_2^-$  tetrahedra in the structure determines the framework charge which is balanced by cations that occupy nonframework positions. A representative empirical formula for a zeolite is written as:



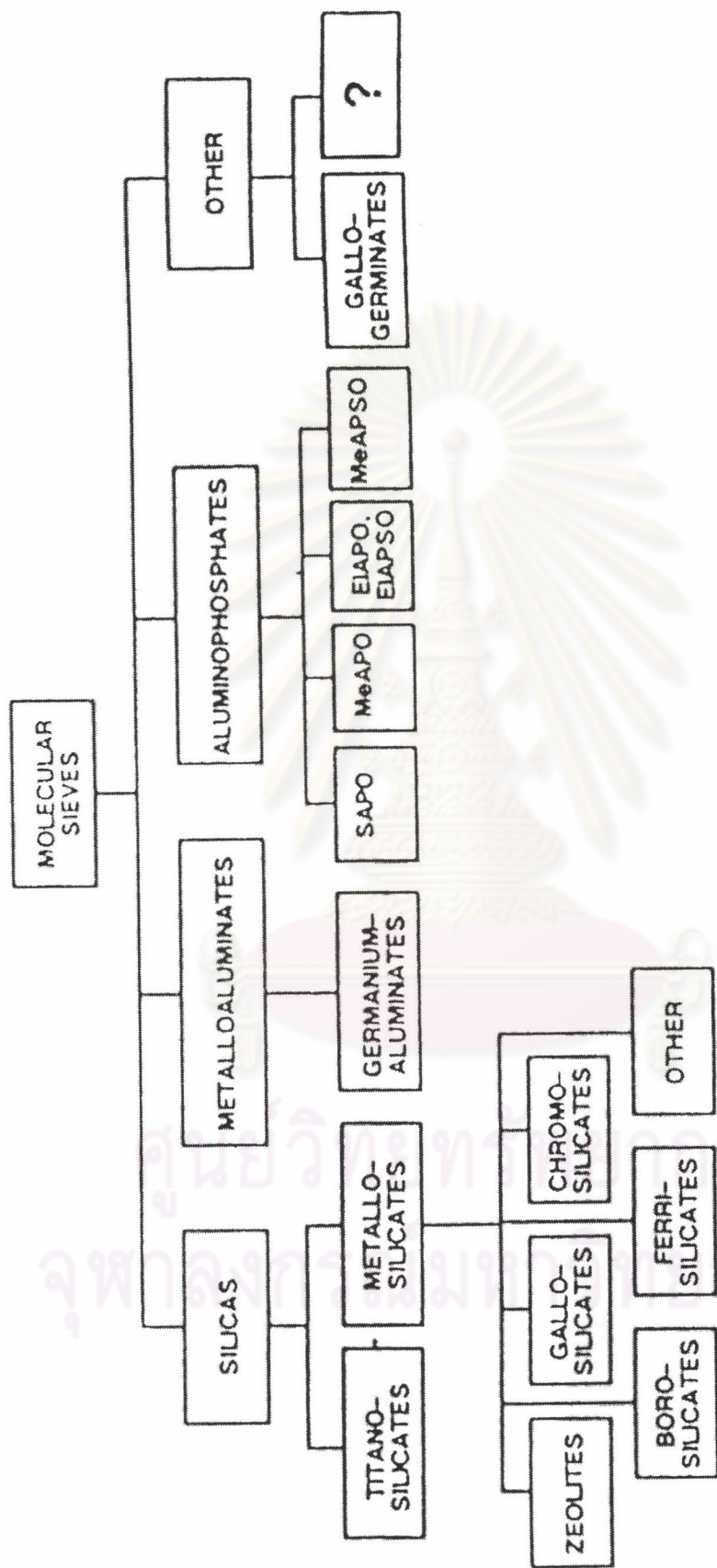
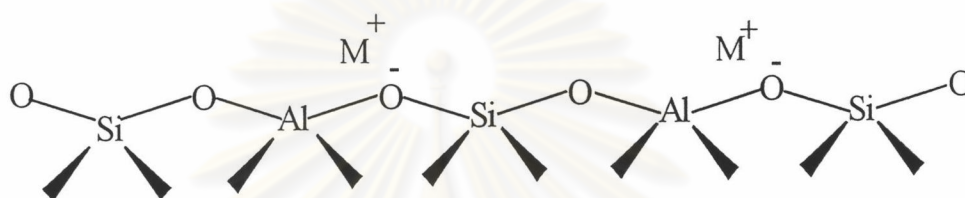


Figure 2.1 Classification of molecular sieve materials indicating the extensive variation in composition. The zeolites occupy a subcategory of the metallosilicates.

where M represents the exchangeable cations, the alkali or alkali earth ions, although other metal, nonmetal, and organic cations may also be used to balance the framework charge, and  $n$  represents the cation valency. These cations are present either during synthesis or through post-synthesis ion exchange. The value of  $y/x$  is equal to or greater than 2 because  $\text{Al}^{3+}$  does not occupy adjacent tetrahedral sites.



The crystalline framework structure contains voids and channels of discrete size. The pore or channel openings range from 3 to 8 Å, depending on the structure. Water molecules present are located in these channels and cavities, so are the cations that neutralize the negative charge created by the presence of the  $\text{AlO}_2^-$  tetrahedra in the structure. Typical cations include the alkaline ( $\text{Na}^+$ ,  $\text{K}^+$ ,  $\text{Rb}^+$ ,  $\text{Cs}^+$ ) and the alkaline earth ( $\text{Mg}^{2+}$ ,  $\text{Ca}^{2+}$ ) cations,  $\text{NH}_4^+$ ,  $\text{H}_3\text{O}^+$  ( $\text{H}^+$ ),  $\text{TMA}^+$  (tetramethylammonium) and other nitrogen-containing organic cations, and the rare-earth and noble metal ions.

### 2.2.1 Structures of Zeolites

Describing zeolites in terms of their pore openings and channel systems simplifies by comparisons of their adsorptive and catalytic properties. The need to comprehend, or at least relate, the seemingly large number of complex zeolite structures in order to compare structural properties has led to the development of structural building units.

The primary building unit of a zeolite structure is the individual tetrahedral  $\text{TO}_4$  unit, where T is either Si or Al. Figure 2.2 represents the primary building unit of the zeolite.

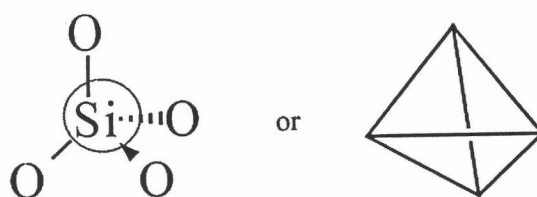


**Figure 2.2** The primary building unit of the zeolite.

A secondary building unit (SBU) consists of selected geometric groupings of those tetrahedra. There are nine such building units, which can be used in describing all of known zeolite structures. These secondary building units consist of 4-, 6-, and 8-member single rings, 4-4, 6-6, and 8-8 member double rings, and 4-1, 5-1, and 4-4-1 branched rings. The topologies of these units are shown in Figure 2.3. Also listed are symbols used to describe them. Most zeolite frameworks can be generated from several different SBU's. Descriptions of known zeolite structure based on their SBU's are listed in Table 2.1. The framework structures of some zeolites are shown in Figure 2.4.

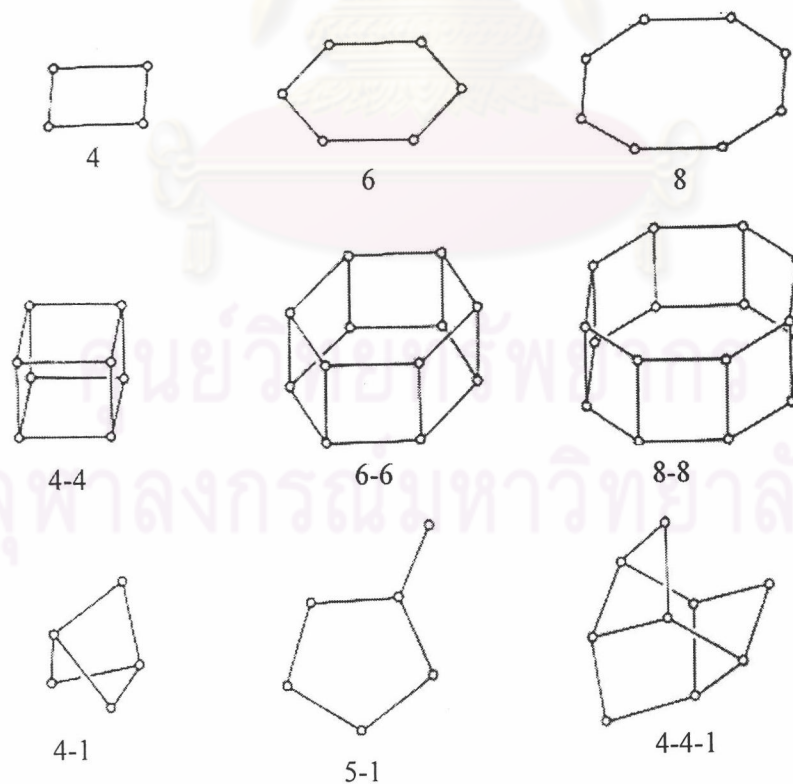


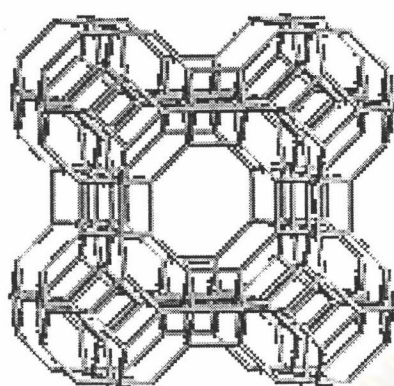
**Figure 2.3** Secondary building units found in zeolite structures.



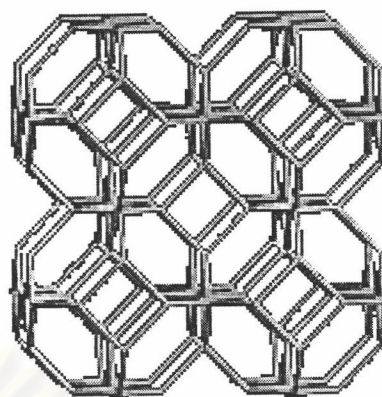
**Table 2.1** Zeolites and their secondary building units. The nomenclature used is consistent with that presented in Figure 2.3

Zeolite	secondary building units								
	4	6	8	4-4	6-6	8-8	4-1	5-1	4-4-1
Analcime	X	X							
ZSM-5								X	
Mordenite								X	
Sodalite	X	X							
Type A	X	X	X	X					
Stilbite									X
Cancrinite							X		
Faujasite	X	X			X				
Chabasite	X	X			X				
Merlionite	X		X			X			

The secondary building unit does provide convenient method of topologically describing and relating different zeolites. However, in many instances describing structural differences and similarities requires a building unit that takes into account the arrangement of these secondary building units in space. The chain-building unit adds further dimension to the building unit. There are in fact four unique orientations for the tetrahedra in 4-member ring. All four tetrahedral can be pointing up (or all four pointing down), two adjacent can be pointing up with the either two pointing down, the two opposite tetrahedra can be pointing up, or three can be pointing up. The development of chain formed from these 4 member-rings structural building units is depicted in Figure 2.5.



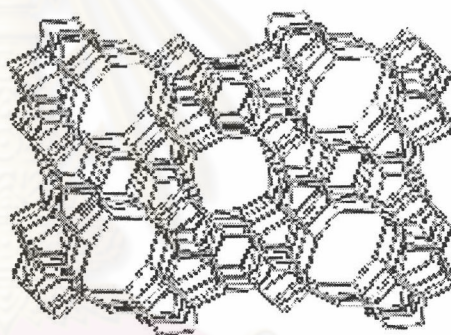
Zeolite A



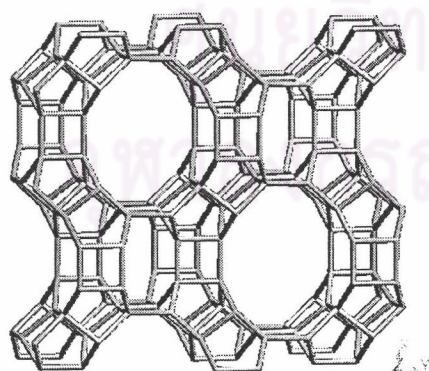
Sodalite



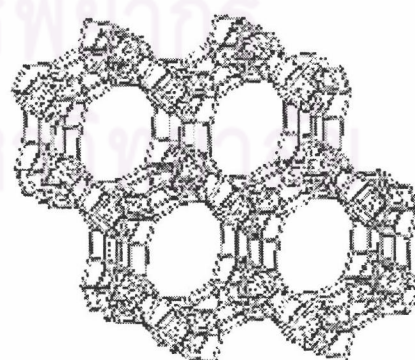
Zeolite X, Y



ZSM-5



Mordenite



MEI

**Figure 2.4** Framework structures of some zeolites.

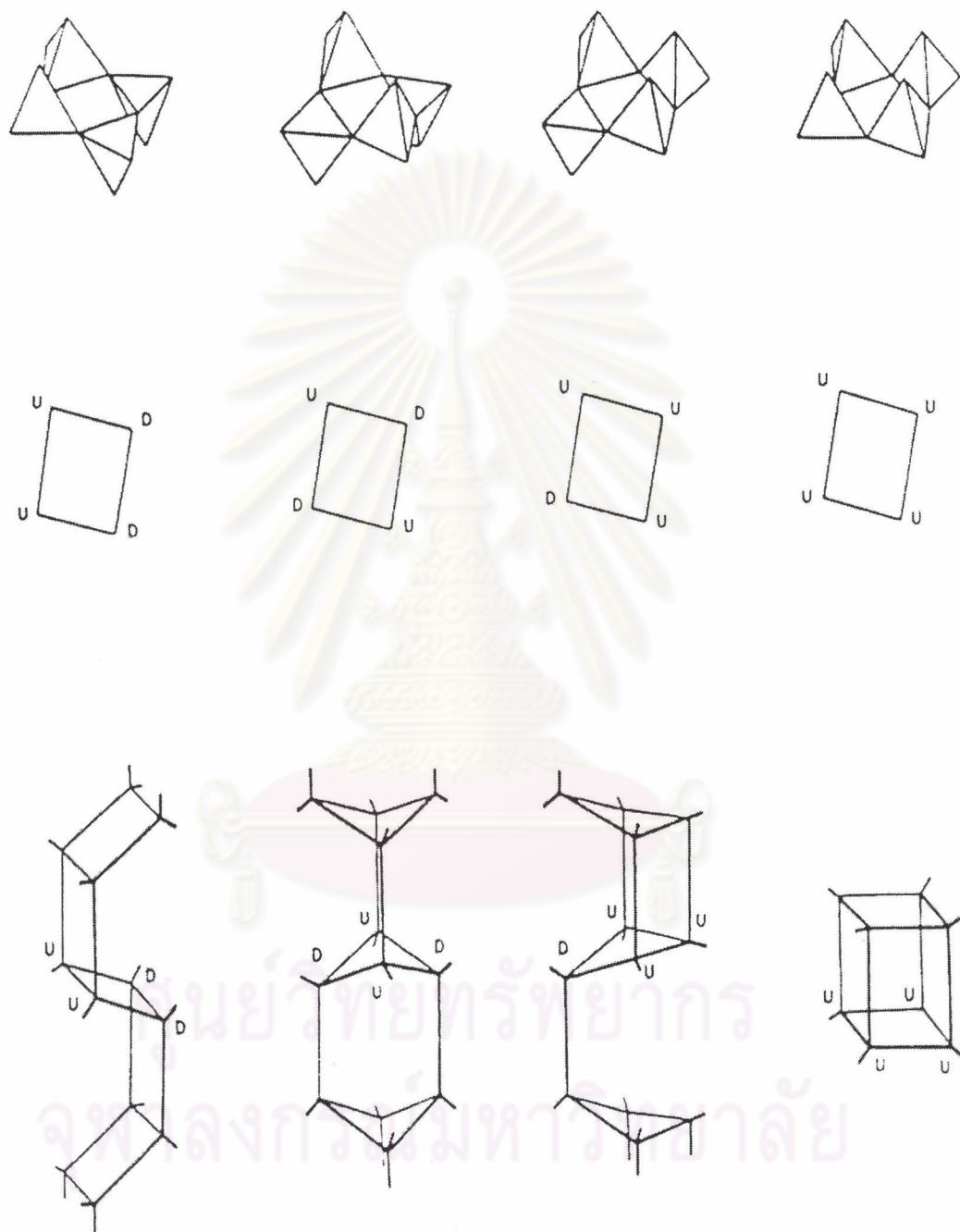


**Figure 2.5** Silicate anions generated by linking rings in different directions of their tetrahedra.



## 2.2.2 Properties of Zeolites

### 2.2.2.1 Shape and Size Selectivity

Shape and size selectivity plays a very important role in catalysis. Highly crystalline and regular channel structures are among the principal features that molecular sieves used as catalysts offer over other materials.

There are three types of shape selectivity: reactant shape selectivity, product shape selectivity, and transition-state shape selectivity. These types of selectivities are depicted in Figure 2.6. Reactant shape selectivity results from the limited diffusion of some of the reactants, which cannot effectively enter and diffuse inside the crystal. Product shape selectivity occurs when slowly diffusing product molecules cannot rapidly escape from the crystal, and undergo secondary reactions. Restricted transition-state shape selectivity is a kinetic effect arising from the local environment around the active site, i.e. the rate constant for a certain reaction mechanism is reduced if the necessary transition state is too bulky to form readily.

The critical diameter (as opposed to the length) of the molecules is important in predicting shape selectivity. However, molecules are deformable and can pass through smaller openings than their critical diameter. Hence not only size but also the dynamics and structure of the molecules must be taken into account.

An equivalent to activation energy exists for the diffusion of molecules inside the molecular sieve because the temperature-dependent translational energy of molecule (as move through the force fields in the pores) must increase significantly as the dimensions of the molecular configuration approach the void dimensions of the crystal. It should be noted that the effective diffusivity varies with molecular type; adsorption affinity affects diffusivity, and rapidly reacting molecules (such as olefins) show diffusional mass-transfer limitations inside the structure due to their extreme reactivity.



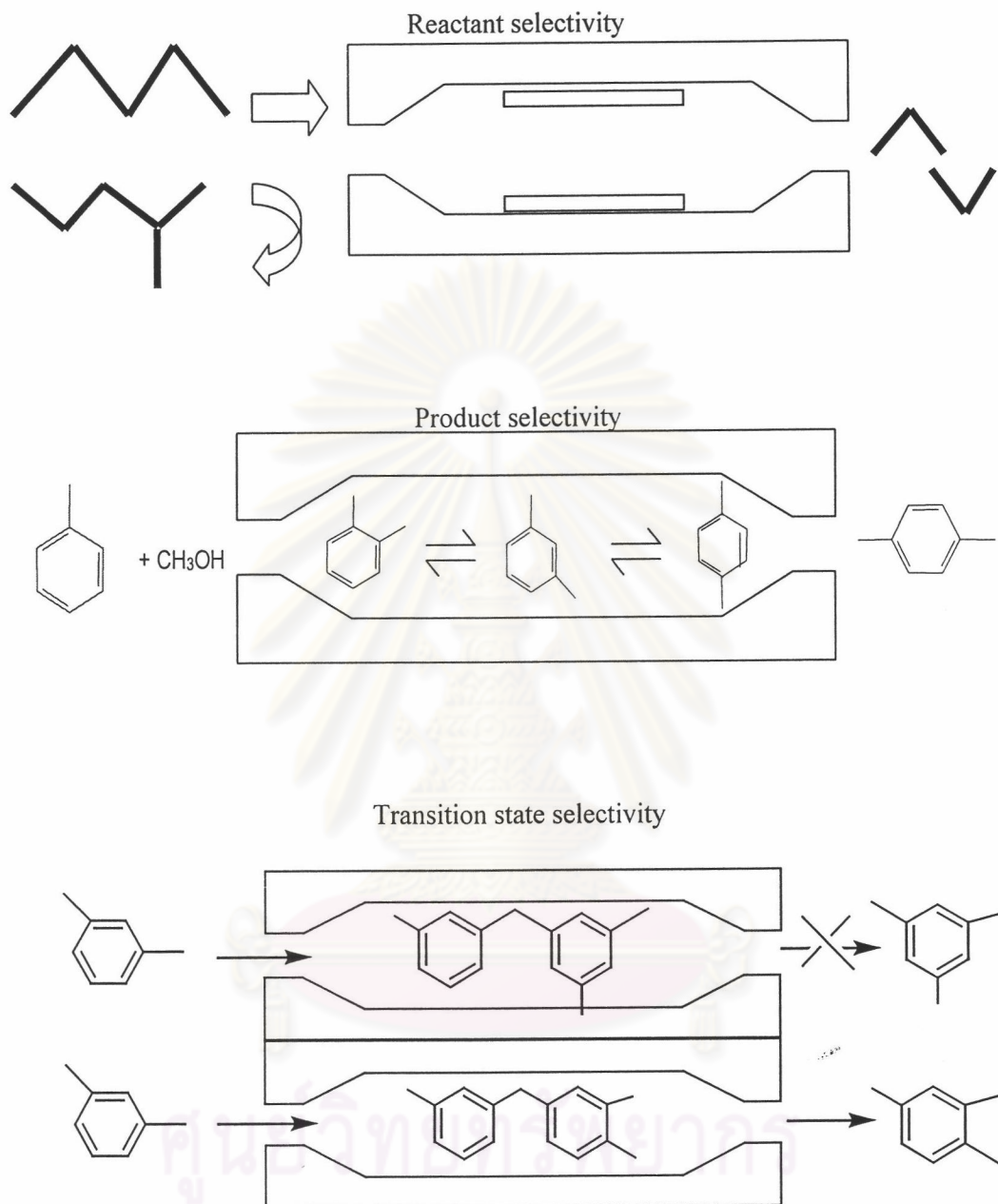


**Figure 2.6** Diagram depicting the three types of selectivity: reactant, product, and transition state shape selectivity.

The effective size and relative accessibility of the pore and cavities can be altered by partially blocking the pore and/or by changing the molecular sieve crystal size. Effect of shape selective are especially induced by the above two methods when the diffusivities of these species differ significantly.

### 2.2.2.2 Cation-Exchange

On the surface of the zeolite, there are the cations that neutralize the negative charge created by the  $\text{AlO}_2^-$  tetrahedra in the structure. Typical cations include, the alkaline ( $\text{Na}^+$ ,  $\text{K}^+$ ,  $\text{Rb}^+$ ,  $\text{Cs}^+$ ) and the alkaline earth ( $\text{Mg}^{2+}$ ,  $\text{Ca}^{2+}$ ) cations. The cations are on the surface that can exchange to the other cations that are shown in the Figure 2.7.

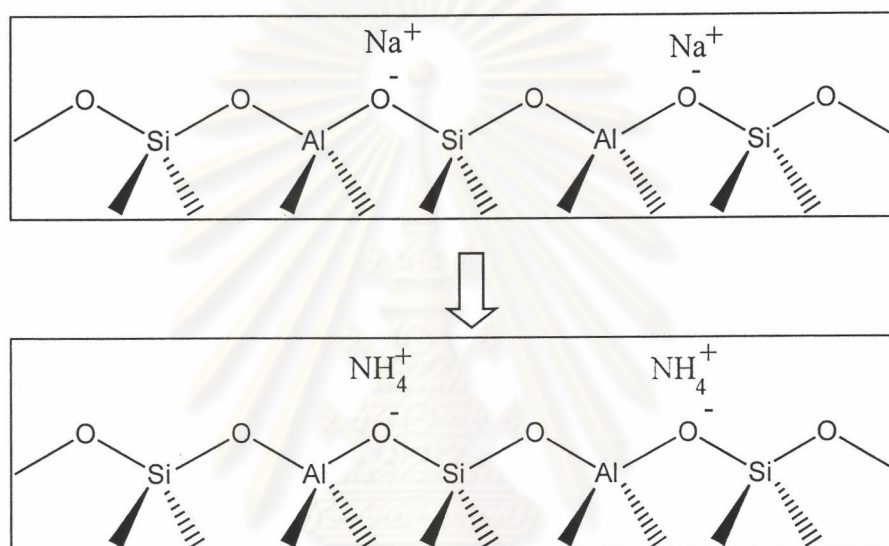


**Figure 2.7** Diagram depicting the cation-exchange on the surface of the zeolite.

### 2.2.2.3 Acid Sites (Acidity)

All of the variation pretreatment conditions as well as synthesis and post-treatments (hydrothermal, thermal and chemical), affect the ultimate acidity an activity observed in the zeolite molecular sieves. Both Brønsted and Lewis acid sites are exhibited in these materials, with assertions by various investigation that:

1. Brønsted acid sites are the active center.
2. Lewis acid sites are the active center.
3. Brønsted and Lewis acid sites together act as the active centers.

4. Cations or the other types of sites in small concentrations act in the conjunction with the Brønsted/Lewis acid sites to function as the active center.

Strong electric fields in the zeolites arise from the various charge species. This is Brønsted/Lewis acidity model usually employed to describe the active sites of molecular sieves. Figure 2.8 depicts a zeolite structure with Brønsted and Lewis acid sites.

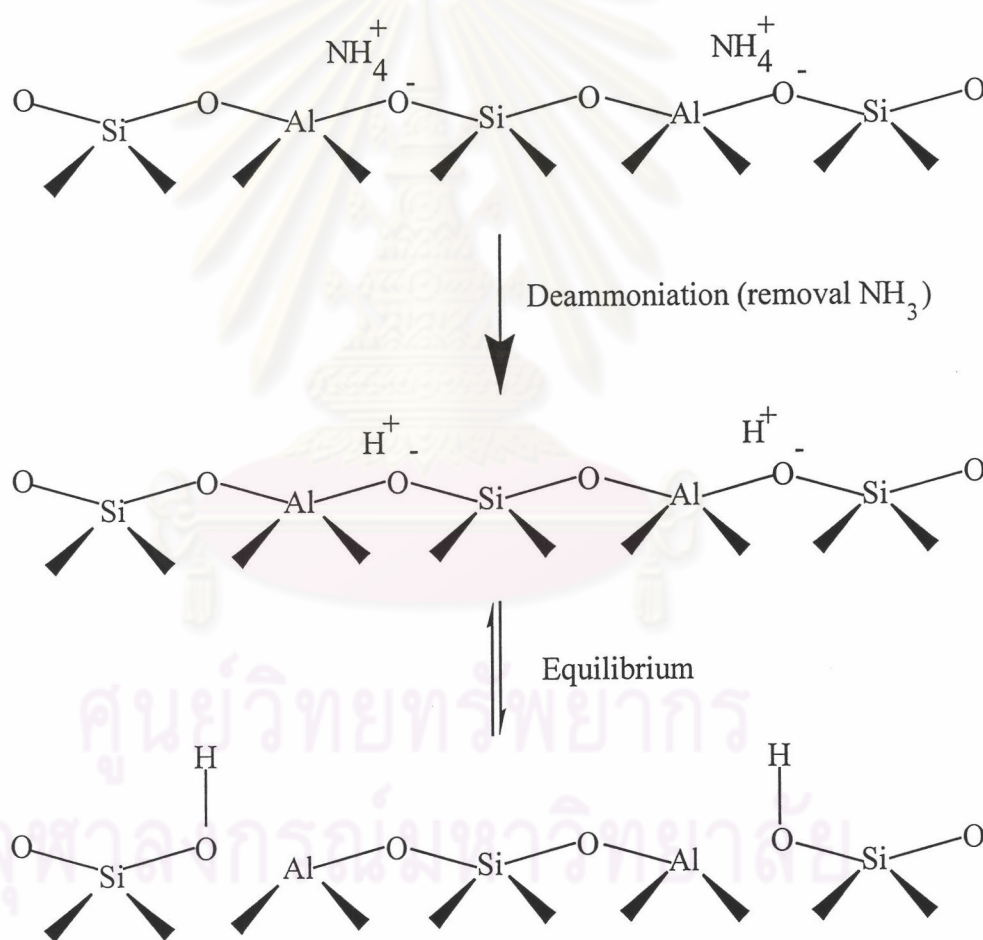


**Figure 2.8** Diagram of the “surface” of a zeolite framework.

The ammonium-form zeolite was converted to the hydrogen-form one by calcinations at elevated temperature. The thermal treatment causes removal of  $\text{NH}_3$

from the cation sites and leaves protons as the balancing cations. The aluminum sites with its associated bridged Si-O-H are a classical Brønsted acid. The Brønsted acid site has been proposed to exist in equilibrium with the so call Lewis acid site, the trigonally coordinated aluminum.

Dealumination by acid treatment results in material having similar properties with dealuminated zeolites resulting from dehydroxylation as shown in Figure 2.9. In general, chemical treatments, including acid extraction of aluminum from zeolite framework, usually affect the external surface of crystal. Hydrochloric acid treatment, for example, removes aluminum to yield a silica-rich external surface.

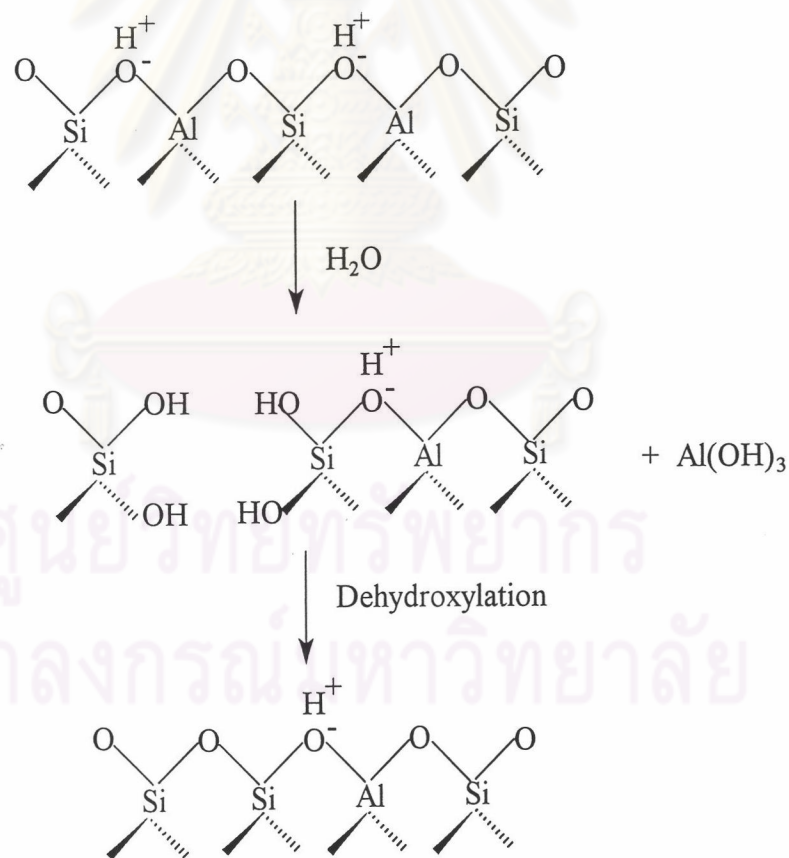


Figure 2.9 The mechanism of framework dealumination.



The products of dealumination can be extracted from the molecular sieve pores by the use of acid. However, the removal of the aluminum from the lattice has been claimed to produce a “nest” of four Si-O-H silanols. Dehydroxylation is believed to be accomplished at the area of the silinol “nest”, followed by reconnection of Si-O-Si bonds. As a result the unit cell of zeolites is contracted.

### 2.3 Structure and Chemical Properties of the Mordenite Zeolite

Mordenite<sup>2-3</sup> is one of large-pore zeolites that occurs readily in nature. The mordenite zeolite has two different pores. Its SBU of six tetrahedral is called the 5-1 unit and each tetrahedron belongs to one or more 5-member rings in the framework. Mordenite is a large-pore zeolite having an orthorhombic crystalline structure. The structure consists of chains that are crosslinked by the sharing of neighboring oxygens. The high degree of thermal stability shown by mordenite is probably due to the large number of 5-member rings that are energetically favored in terms of stability. The larger pore is 12-member ring of the size  $6.7 \text{ \AA} \times 7.0 \text{ \AA}$  and its smaller pore is 8-member ring of the size  $2.9 \text{ \AA} \times 5.7 \text{ \AA}$ . The framework structure of mordenite is shown in Figure 2.10.

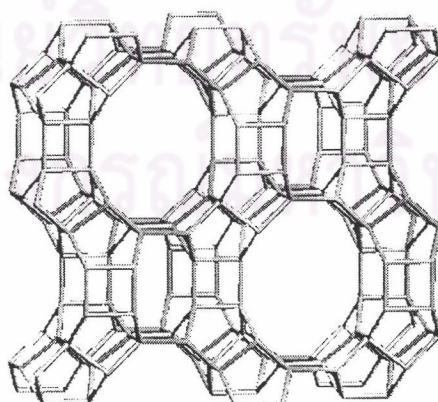


**Figure 2.10** The framework structure of mordenite.

The chemical formula of a typical unit cell of hydrated Na-mordenite ( $\text{Si/Al} = 5$ ) is  $\text{Na}_8[(\text{AlO}_2)_8(\text{SiO}_2)_{40}]\cdot 24\text{H}_2\text{O}$ . In the hydrated crystal, 4 sodium ions have been located in the constrictions with a minimum diameter of 2.8 Å. Locations of the remaining 4 sodium ions and water molecules are not known. Large cations such as cesium cannot occupy the positions determined for sodium. Natural mordenite contains crystal stacking faults in the  $c$  direction or amorphous material or cations in the channels that severely restrict diffusion into the large channel system. Many of the synthetic mordenite do not exhibit such pore restriction.

## 2.4 Characterization of Zeolites

### 2.4.1 X-ray Diffraction of the Mordenite Zeolite

X-ray powder diffraction patterns of zeolites and molecular sieves are fingerprints of their structures. From Bragg's law, when an X-ray beam strikes a crystal surface at some angle ( $\theta$ ), a portion of the beam is scattered by the layer of atoms at the surface. The unscattered portion of the beam penetrates to the second layer of atoms and the third layer of atom, respectively. The diffraction of X-ray by the crystal is shown in Figure 2.11. When atoms are located in crystal at the same interlayer distance, this diffraction is similar to the diffraction of grating, where  $d$  is the interplanar distance of the crystal. Thus, the conditions for constructive interference of the beam at angle  $\theta$  are called Bragg equation.

$$n\lambda = 2d \sin\theta$$

The typical X-ray diffraction data for the mordenite zeolite are shown in Table 2.2 and its XRD pattern is shown in Figure 2.12. The X-ray diffraction data include the spacing ( $d$ ) and the relative intensity ( $I$ ). The spacing ( $d$ ) is given in angstrom units, and  $I$  is the peak intensities relative to the strongest peak in the pattern ( $I_0=100$ ).

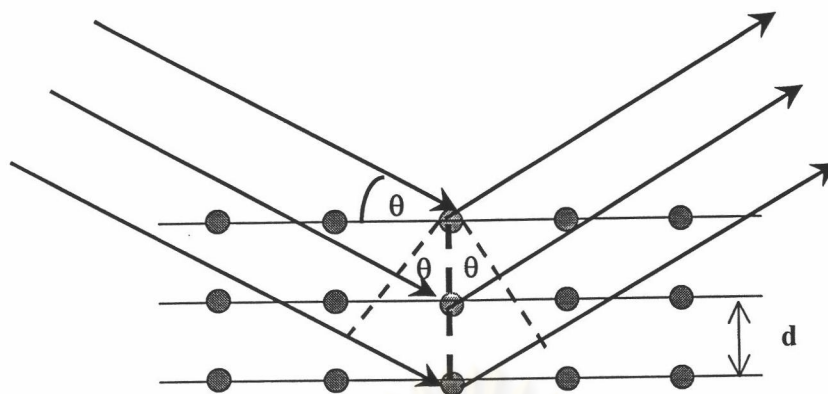


Figure 2.11 Diffractions of X-rays by a crystal.

Table 2.2 XRD data for the mordenite zeolite with the typical unit cell:



d(Å)	2θ	I	d(Å)	2θ	I
13.581	6.51	100	3.245	12.6	12.6
10.265	8.61	13.1	3.223	27.67	46.1
9.055	9.055	56.4	3.201	27.87	28.8
6.584	13.45	40.4	2.946	30.34	5.5
6.402	13.83	29.1	2.894	30.89	12.9
6.071	14.59	13.3	2.894	30.89	8.8
5.791	15.30	9.5	2.702	33.15	6.6
4.527	19.61	22.7	2.566	34.96	5.4
4.142	21.45	5.7	2.521	35.61	15.5
1.004	22.2	46.1	2.459	36.54	5.3
3.840	23.16	16.9	2.053	44.11	5.3
3.764	23.64	6.9	2.018	44.92	4.9
3.476	25.63	75.7	1.955	46.44	7.3
3.422	26.04	5.0	1.920	47.34	5.2
3.395	26.25	43.5	1.882	48.36	9.4

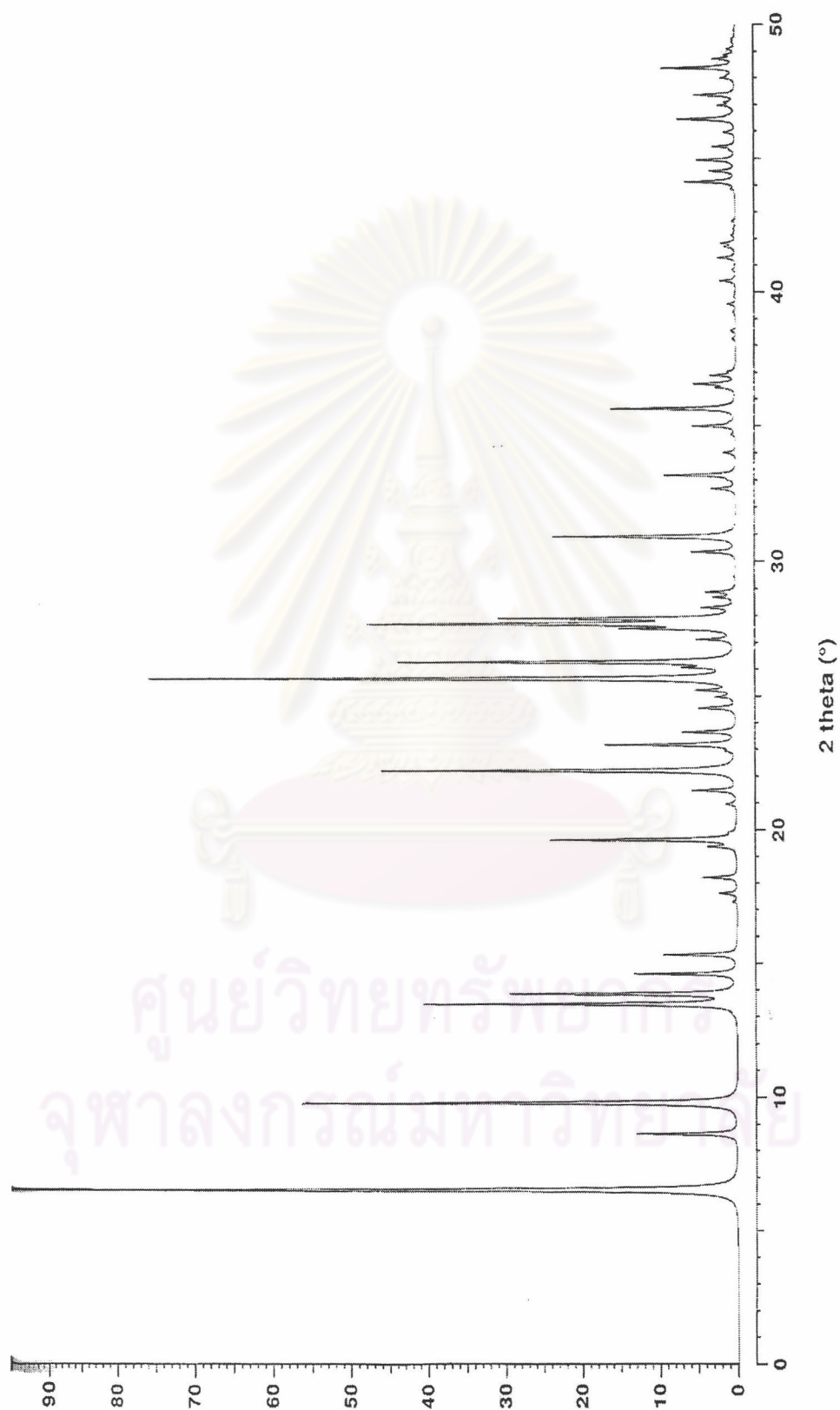


Figure 2.12 XRD pattern for the mordenite zeolite.<sup>33</sup>



### 2.4.2 Atomic Absorption Spectroscopy

Atomic absorption is one method to determine Si/Al ratio in a zeolite. A number of atoms are obtained from the absorption of free atoms at their characteristic wavelength. For example, the sodium atom absorbs radiation at a wavelength of 589 nm to transmit, in contrast calcium atom absorbs radiation at the wavelength of 423 nm. Energy absorbed by an atom may be thermal energy. When the atom absorbs thermal energy, dissociation, vaporization, ionization or excitation of the atom occurs.

For monochromatic radiation, absorbance is directly proportional to the path length  $b$  through the medium and the concentration  $c$  of the absorbing species with the molar absorptivity  $\epsilon$ .

$$A = \epsilon bc$$

These relationships are expressions of Beer's law, which serves as the basis for quantitative analyses. The Attenuation of a beam of radiation by an absorbing solution is shown in Figure 2.13.

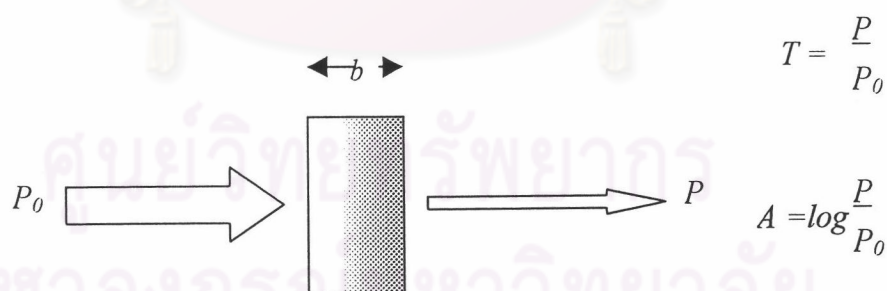


Figure 2.13 The attenuation of a beam of radiation by an absorbing solution.

### 2.4.3 Ammonium Temperature Program Desorption

Temperature-programmed desorption (TPD) of ammonia is probably the most widely used method for characterizing acidity in zeolites and mesoporous materials. There are many variations on the method, but it typically involves saturation of the surface with ammonia

under some sets of adsorption conditions, followed by linear ramping of the temperature of the sample in a flowing inert gas stream. Ammonia concentration in the effluent gas may be followed by absorption/titration or mass spectroscopy. Alternatively, the experiment may be carried out in a microbalance and changes in sample mass may be followed continuously. The amount of ammonia desorbing above some characteristic temperature is taken as the acid-site concentration, and the peak desorption temperatures have been used in calculation for heats of adsorption. The temperatures are corresponding to the strength of ammonia-acid interaction as well.

#### 2.4.4 Solid State $^{27}\text{Al}$ -MAS-NMR

Another important characterization technique for zeolites is solid state NMR.  $^{27}\text{Al}$  MAS-NMR spectroscopy has been employed to distinguish between tetrahedrally and octahedrally coordinated aluminum (at approx. 56 and 0 ppm, respectively). Hence, the relative amount of framework aluminum can be determined.

## 2.5 Catalytic Cracking

Endothermic catalytic cracking of hydrocarbons, particularly petroleum fractions, to lower molecular weight desirable products is well known.<sup>34</sup> This process is practiced industrially in a cycling mode wherein hydrocarbon feedstock is contacted with hot, active, solid particulate catalyst without added hydrogen at rather low pressures of about 50 psig and temperatures sufficient to support the desired cracking. As the hydrocarbon feed is cracked to lower molecular weight, more valuable and desirable products, coke is deposited on the catalyst particles. Coke is burned off from the catalyst particles to regenerate the catalytic activity.

Two major variants for endothermically cracking hydrocarbons are fluid catalytic cracking (FCC) and fixed bed catalytic cracking. Cracking catalysts which may be a crystalline aluminosilicate zeolites and amorphous silica alumina.<sup>1,15-17</sup> For catalytic cracking,

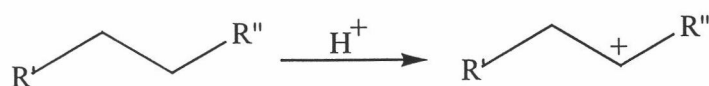
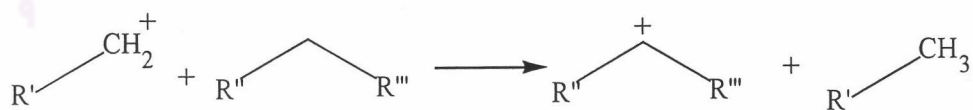
the acidity of the zeolite affects the catalytic activity of the zeolite. In general, when the Si/Al molar ratio in zeolite increases, the acidity of the zeolite also decreases. The acidity of the zeolite depends on Brønsted and Lewis acid sites. The activities for polymer degradation over zeolites increase when the acidity of the zeolites increases. However the best catalytic condition is not received when the Si/Al ratio increases, the best condition is obtained when the acidity of zeolite is optimized. For example, Seo *et al.*<sup>4</sup> reported the optimum for polyethylene wax degradation over zeolite mordenite at the temperature of 380°C was using zeolite mordenite with the Si/Al ratio of 12 as catalyst.

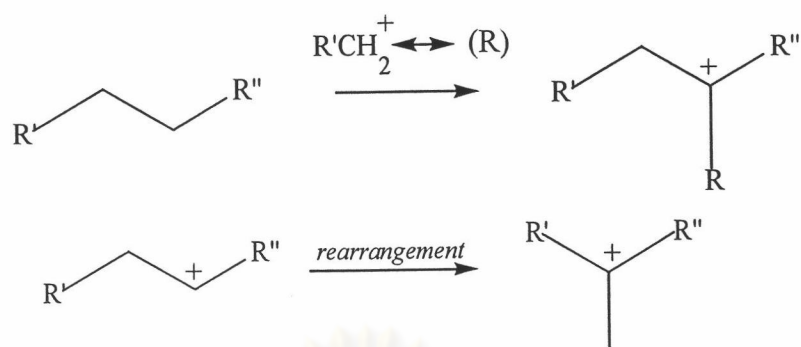
### 2.5.1 Mechanism of Catalytic Cracking of Polyethylene

A mechanism of the degradation of polyethylene was proposed.<sup>34-35</sup> The protons from Brønsted acid catalysts can attack polymer chains resulting in formation of primary carbenium ions:

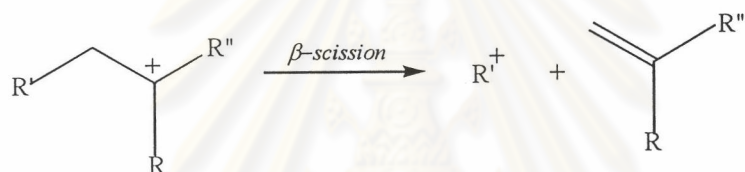


Primary carbenium ions can react via inter- or intramolecular mechanisms to produce secondary carbenium ions, which may rearrange to form more stable tertiary ions:

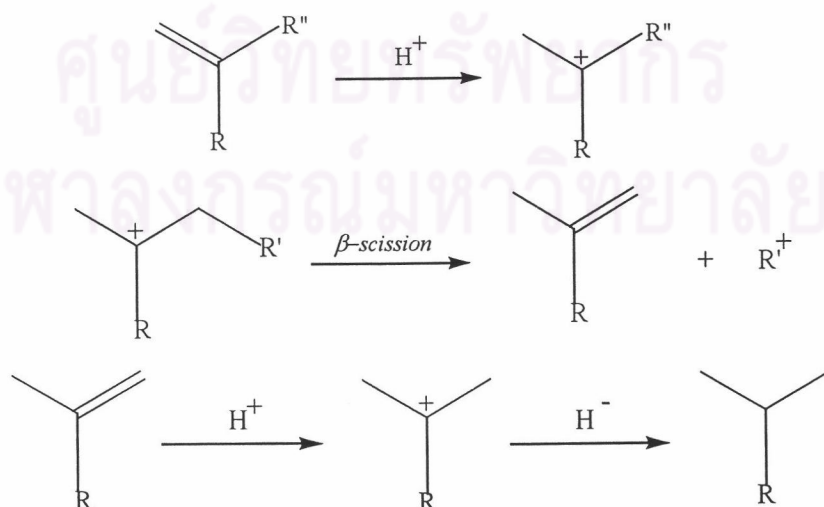




$\beta$ -scission of these secondary and tertiary carbenium ions can result in the formation of new primary carbenium ions and chain-end olefins.



Chain-end olefin double bonds can react with catalyst protons to again form carbenium ions, which, after  $\beta$ -scission, can produce propene or isobutene, depending on whether R in the equation below is H or CH<sub>3</sub>.





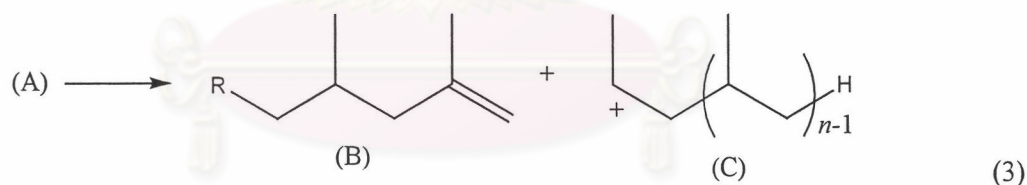
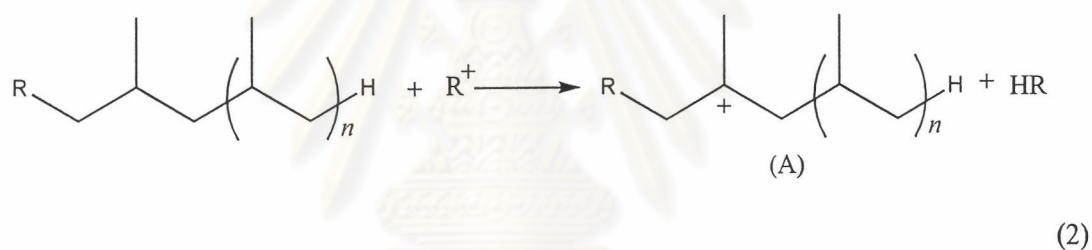
### 2.5.2 Mechanism of Catalytic Cracking of Polypropylene

The degradation of polypropylene mechanism was proposed in several steps.<sup>36</sup>

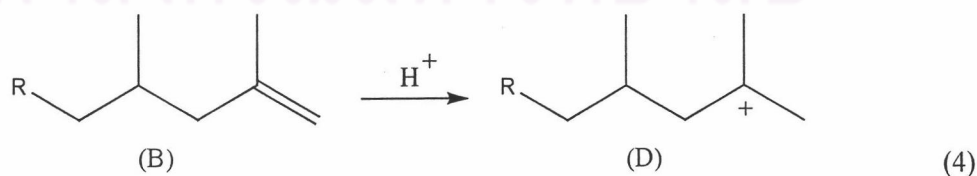
The molecular weight reduction is first initiated by attack of low molecular weight carbenium ions,  $R^+$ , on hydrogen atoms attached to the tertiary carbon atoms of the polypropylene backbone chains. These ions are produced by protonation of volatile olefinic products present in the polymer as impurity, as follows:



where  $R^+$  stands for volatile olefinic products



$\beta$ -scission of on-chain tertiary carbenium ions (A) occurs to produce chain-ends (B) and (C). The protonation of vinylidene (B) occurs to produce tertiary carbenium ions (D) as follows:



Gas formation may occur mainly from the ions (C) and (D). Ion (D) is mainly transformed by hydride ion addition or  $\beta$ -scission to produce chain-ends (E) and isobutene (F). (F) produces isobutane by hydrogenation as follow:



